Spectrochimica Acta Part A: Molecular and Biomolecular Spectroscopy 246 (2021) 118953

Contents lists available at ScienceDirect

Spectrochimica Acta Part A: Molecular and Biomolecular Spectroscopy

journal homepage: www.elsevier.com/locate/saa

A dual-analytes responsive fluorescent probe for discriminative detection of ClO^- and N_2H_4 in living cells

Beitong Zhu [a,b,1], Xiaoli Wu [a,1], João Rodrigues [c], Xichao Hu [a,*], Ruilong Sheng [c,*], Guang-Ming Bao [b,*]

[a] School of Food and Drug, Luoyang Normal University, Luoyang 471934, PR China
[b] Institute of Veterinary Drug, Jiangxi Agricultural University, Nanchang 330045, PR China
[c] CQM-Centro de Quimica da Madeira, Universidade da Madeira, Campus da Penteada, 9000-390 Funchal, Madeira, Portugal

ARTICLE INFO

Article history:
Received 14 August 2020
Received in revised form 6 September 2020
Accepted 9 September 2020
Available online 17 September 2020

Keywords:
Fluorescent probe
Dual-analytes
N_2H_4
ClO^-
Bioimaging
Living cells

ABSTRACT

Hydrazine (N_2H_4) and ClO^- are very harmful for public health, hence it is important and necessary to monitor them in living cells. Herein, we rationally designed and synthesized a dual-analytes responsive fluorescent sensor **PTMQ** for distinguishing detection of N_2H_4 and ClO^-. **PTMQ** underwent N_2H_4-induced double bond cleavage, affording colorimetric and green fluorescence enhancement with good selectivity and a low detection limit (89 nM). On the other hand, **PTMQ** underwent ClO^--induced sulfur oxidation and displayed red fluorescence lighting-up response towards ClO^- with good selectivity, rapid response (<0.2 min) and a low detection limit (58 nM). Moreover, **PTMQ** was successfully employed for in-situ imaging of N_2H_4 and ClO^- in living cells.

1. Introduction

Hydrazine (N_2H_4) is an essential chemical substance, which has been widely used in chemical synthesis and catalysis, as well as in the pharmaceutical industry [1,2]. Hydrazine is generally produced by hypochlorite (ClO^-)-mediated oxidation of ammonia or urea. Hence, the discharged industrial wastewater from hydrazine manufacture usually contains hydrazine and hypochlorite, which would be taken up by aquatic organisms/microorganisms and cause extremely toxic effect on them. Besides, N_2H_4 can cause severe damage to the liver, kidneys, lungs, central nervous system, and the respiratory system. For this reason, N_2H_4 has been categorized into a highly toxic and carcinogenic substance (B_2 grade) by US government [3], and the concentration of N_2H_4 in water should be lower than 10 ppb [4]. Therefore, it is of great importance to monitor hydrazine in living cells/organisms.

Fluorescent probes have emerged as remarkable sensing tools for the detection of cationic, anionic, and biomolecules [5–11] due to the advantages of visual signal output, good selectivity, high sensitivity, and real-time monitoring ability. Up to date, a great many of reaction-based fluorescent probes were adopted for the detection of hydrazine, in which the reactive sites including methylene malononitrile [12], phthalimides [13,14] and carboxylates [15,16] served as hydrazine-specific moieties. Recently, Zeng et al. developed a coumarin-based chemosensor for discriminative detection of hydrazine and bisulfate via hydrazine-induced ethyl cyanoacetate cleavage and bisulfate-involved Michael addition [17]. Likewise, several fluorescent sensors for visual detection of HOCl/ClO^- have been explored on the basis of the ClO^--mediated oxidation reaction of various functional groups such as ether [18], p-methoxyphenol [19], thioether [20,21], oxime [22–24], hydroxamic acid [25] and C═C double bond [26,27]. Although the above-mentioned progresses have been made, until now, two analytes ClO^- and N_2H_4 hardly be distinguishingly determined by using a simple, effective and visible chemosensor.

It is disclosed that integration of two different reaction/binding sites into a single fluorescent probe could be an efficient approach to achieve discriminative detection of two analytes [17,26–28]. In this study, we designed a dual-analytes responsive fluorescent probe **PTMQ** for the distinguishing detection of ClO^- and N_2H_4. Probe **PTMQ** possesses two reaction sites: (1) the sulfur atom (—S—) located at the 9-position of phenothiazine serves as a reaction site for ClO^-; (2) the **MQ** moiety acts as the reactive site for N_2H_4. We anticipated that **PTMQ** would separately react with HClO and N_2H_4, generating fluorescent products with different color/fluorescence signal output. We investigated the colorimetric and fluorescence responses, selectivity and sensitivity, detection limit, as well as time-dependent fluorescence

* Corresponding authors.
E-mail addresses: hxc30@163.com (X. Hu), ruilong.sheng@staff.uma.pt (R. Sheng), bycb2005@gmail.com (G.-M. Bao).
[1] These authors contributed equally to this work.

https://doi.org/10.1016/j.saa.2020.118953
1386-1425/

response of **PTMQ** to ClO^- and N_2H_4, respectively. Moreover, **PTMQ** was used to in-situ image ClO^- and N_2H_4 in living human cervical cancer HeLa cells.

2. Experimental

2.1. Chemicals and instrumentations

All chemicals were commercially purchased from Sigma-Aldrich and used directly without further purification. Compound **1** (N-ethyl-4-methylquinolinium iodide, **MQ**) was prepared according to the literature [29]. ^{1}H NMR (400 MHz) and ^{13}C NMR (100 MHz) spectra were measured on a Bruker AV spectrometer. High resolution mass spectrometry (HRMS) was obtained on HP-1100 LC-MS spectrometer. UV–Vis absorption spectra were performed on a Hitachi UV-3310 spectrometer. Fluorescence spectra were obtained with a FL-4500 fluorescence spectrometer. The cells imaging experiments were taken under a Nikon A1 confocal laser-scanning microscope with a 100 × objective lens.

2.2. Synthesis of compound **2** (N-propagyl-8-methoxy-phenothiazine)

In a 250 mL flask, 2-methoxyphenothiazine (500 mg, 2.18 mmol), 3-bromopropyne (1.30 g, 10.90 mmol) and KI (166 mg, 1.0 mmol) were dissolved in 15 mL anhydrous DMF. The mixture was stirred at 100 °C for 8 h under N_2 atmosphere. After cooling down to room temperature, the resulted mixture was poured into 100 mL H_2O and extracted three times with CH_2Cl_2. Then, solvent of the collected organic layer was removed under reduced pressure. The obtained crude product was further purified by silica gel flash chromatography (petroleum ether/ethyl acetate = 15:1, v/v) to give compound **2** (N-propagyl-8-methoxy-phenothiazine) as colorless solid (495 mg, yield: 85%). ^{1}H NMR (400 MHz, DMSO-d_6) δ 7.24 (t, J = 7.7 Hz, 1H), 7.21–7.12 (m, 2H), 7.07 (d, J = 8.4 Hz, 1H), 6.99 (t, J = 7.4 Hz, 1H), 6.79 (s, 1H), 6.62 (d, J = 8.4 Hz, 1H), 4.64 (s, 2H), 3.76 (s, 3H), 3.50 (s, 1H). ^{13}C NMR (100 MHz, DMSO-d_6) δ 159.9, 145.4, 143.8, 127.9, 127.7, 127.2, 123.4, 123.1, 115.6, 113.2, 107.8, 103.4, 79.9, 77.4, 55.8, 38.0.

2.3. Synthesis of compound **3** (N-propagyl-8-methoxy-phenothiazine-7-aldehyde, **PT**)

Phosphorous oxychloride (0.52 mL, 5.61 mmol) was dropwise added to anhydrous dimethylformamide (0.43 mL, 5.61 mmol) at 0 °C under a N_2 atmosphere. After the mixture was stirred at 0 °C for 30 min, compound **2** (300 mg, 1.12 mmol) in 5 mL anhydrous dimethylformamide was dropwise added to the above solution. The reacting mixture was heated to 60 °C and stirred for 5 h. Then the resulting mixture was poured into ice water, and the reaction solution was neutralized to pH 7 by NaOH solution (20%) until a large amount of solid precipitated. After filtration, the solid was washed with distilled water (3 × 10 mL), and dried in vacuum and then recrystallized from ethanol to offer compound **3** (N-propagyl-8-methoxy-phenothiazine-7-aldehyde, **PT**) as yellow solid (252 mg, yield: 78%). ^{1}H NMR (400 MHz, DMSO-d_6) δ 10.14 (s, 1H), 7.40 (s, 1H), 7.32–7.26 (m, 1H), 7.24 (d, J = 8.3 Hz, 1H), 7.21 (d, J = 6.2 Hz, 1H), 7.06 (t, J = 8.1 Hz, 1H), 6.91 (s, 1H), 4.83 (s, 2H), 3.97 (s, 3H), 3.58 (s, 1H)·^{13}C NMR (100 MHz, DMSO-d_6) δ 186.8, 162.6, 151.0, 142.2, 128.3, 127.4, 125.9, 124.5, 122.3, 119.7, 116.3, 113.6, 100.3, 79.3, 77.9, 56.5, 38.6.

2.4. Synthesis of probe **PTMQ**

Compound **1** (**MQ**, 380 mg, 1.27 mmol) and compound **3** (**PT**, 250 mg, 0.85 mmol) were dissolved in 15 mL anhydrous EtOH. Afterward, piperidine (0.1 mL) and AcOH (0.1 mL) were added to the solution as catalysts. The mixture was refluxed at 80 °C for 6 h under nitrogen atmosphere. Precipitate was formed after cooling down to room temperature. The precipitate was collected by filtration, followed by recrystallization in ethanol to give **PTMQ** as purple solid (332 mg, yield: 68%). ^{1}H NMR (400 MHz, DMSO-d_6) δ 9.26 (d, J = 6.6 Hz, 1H), 9.03 (d, J = 8.6 Hz, 1H), 8.52 (d, J = 8.9 Hz, 1H), 8.41 (d, J = 6.6 Hz, 1H), 8.25 (d, J = 7.2 Hz, 1H), 8.20 (d, J = 5.8 Hz, 2H), 8.03 (s, 2H), 7.30 (t, J = 7.7 Hz, 1H), 7.25 (d, J = 7.8 Hz, 2H), 7.10–7.04 (m, 1H), 6.94 (s, 1H), 4.99 (d, J = 7.2 Hz, 2H), 4.83 (s, 2H), 4.01 (s, 3H), 3.59 (s, 1H), 1.57 (t, J = 7.1 Hz, 3H). ^{13}C NMR (100 MHz, DMSO-d_6) δ 159.0, 153.4, 147.9, 147.3, 142.8, 138.1, 136.5, 135.5, 129.4, 128.2, 127.42, 127.2, 127.1, 126.6, 124.2, 122.4, 119.4, 119.2, 118.1, 116.3, 116.1, 113.8, 100.3, 79.5, 77.8, 56.6, 52.4, 38.0, 15.6. HR-MS (ESI, m/z): calcd. for $[C_{29}H_{25}N_2OS]^+$: 449.1682; found: 449.1699.

2.5. General procedures for spectral measurements

10 μM of **PTMQ** solution in DMSO/PBS (v/v = 2/8, pH = 7.4) was used for spectral measurements. Optical tests of **PTMQ** for ClO^- and N_2H_4 were performed as follows: a) **PTMQ** (10 μM) was pre-incubated with ClO^- for 5 min at room temperature. The UV–Vis absorption and the fluorescence spectra were recorded directly. Excitation wavelength was 460 nm with slit widths 5/5 nm; b) **PTMQ** (10 μM) was pre-incubated with N_2H_4 for 30 min at room temperature. Then the UV–Vis absorption and the fluorescence spectra were measured directly. Excitation was at 360 nm with slit widths 2.5/5 nm.

2.6. Fluorescence imaging of ClO^- and N_2H_4 by **PTMQ** in HeLa cells

HeLa cells were seeded in glass-bottomed dishes and cultured in DMEM culture medium with 10% FBS at 37 °C for 24 h. For imaging ClO^- and N_2H_4, the HeLa cells were washed with PBS three times to remove culture medium and then pre-treated with **PTMQ** (10 μM) for 30 min. Afterwards, the cells-containing dishes were washed there times with PBS, and mounted on the stage of confocal laser-scanning microscope. Before fluorescence imaging, the HeLa cells were further co-incubated with different concentrations of ClO^- and N_2H_4 for another 30 min, respectively.

3. Results and discussion

3.1. Design and synthesis of **PTMQ**

Herein, a simple synthetic route was established to prepare the desired dual-analytes responsive fluorescent probe **PTMQ**, as depicted in Scheme 1. 4-Methyl-quinoline was quaternized with ethyl iodide to prepare N-ethyl-4-methyl-quinolinium iodide (compound **1**, **MQ**) via *N*-alkylation reaction. The fluorescent precursor 8-methoxy-phenothiazine was coupled with propagyl bromide to prepare compound **2**, which underwent a Vilsmeier reaction ($POCl_3$/DMF) to prepare N-propagyl-8-methoxy- phenothiazine-7-aldehyde (compound **3**, **PT**). Furthermore, **MQ** reacted with **PT** to prepare the dual-analytes responsive fluorescent probe **PTMQ** via one-step condensation approach. The structure of **PTMQ** was analyzed by ^{1}H NMR, ^{13}C NMR and HR-MS (shown in Figs. S1–S7, Supporting information).

3.2. Sensing performance of **PTMQ** for ClO^- and N_2H_4

The UV–Vis and fluorescent spectra titration of **PTMQ** with HClO and N_2H_4 were measured, respectively (Figs. 1 and 2). As shown in Fig. 1, **PTMQ** itself is non-fluorescence in DMSO/PBS solution due to the strong intramolecular charge transfer (ICT) effect from sulfur (—S—) and nitrogen (—N—) atoms in phenothiazine to quinolinium [30]. Upon the addition of an increasing amount of ClO^-, the absorption band of **PTMQ** at 518 nm gradually decreased with the increase of a new band at 465 nm, and simultaneously the color of the **PTMQ** solution turned from deep purple to light pink. The isosbestic point in the absorption titration spectra implied that **PTMQ** has transformed to a new compound

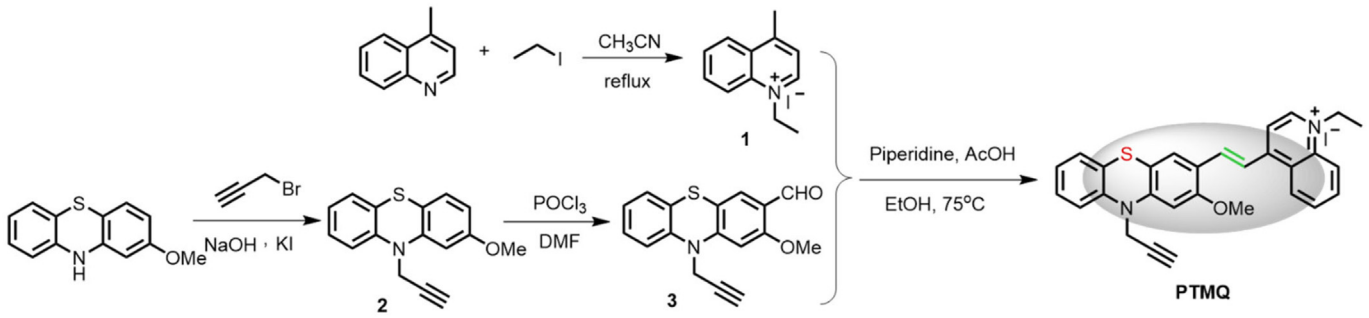

Scheme 1. Synthetic route of probe **PTMQ**

after reaction with ClO^-. Meanwhile, a fluorescence band at 577 nm was lighted-up, which progressively rose up with the increasing amount of ClO^- from 0 to 500 μM (Fig. 1B). Notably, a good linear correlation between fluorescence intensity at 577 nm (F_{577}, $R^2 = 0.9912$) and concentration of ClO^- (0–500 μM) was observed (Fig. 1C), and the detection limit was calculated as 58 nM (S/N = 3). Moreover, the time-dependent fluorescence profile showed that F_{577} of **PTMQ** quickly rose up and reached a stable plateau within 12 s (0.2 min) after addition of ClO^- (500 μM). This observation suggests that **PTMQ** could be used as a rapid-response probe for ClO^- detection in aqueous solution.

The spectral responses of **PTMQ** towards N_2H_4 were shown in Fig. 2. With the addition of increasing amount of N_2H_4, the absorption band of **PTMQ** at 518 nm gradually decreased along with the increase of a new band at 285 nm, and the color of **PTMQ** solution changed from deep purple to colorless in synchrony. Notably, a green fluorescence band emerged at 500 nm, which were becoming much stonger with the increase of N_2H_4 amount from 0 to 900 μM (Fig. 2B). Likewise, a perfect linear correlation between fluorescence intensity at 500 nm (F_{500}, $R^2 = 0.9930$) and N_2H_4 concentration (0–900 μM) was observed (Fig. 2C), and the detection limit was calculated as 89 nM (S/N = 3). From the time-dependent fluorescence enhancement profile, it could be observed that after the addition of N_2H_4 (900 μM), F_{500} of **PTMQ** gradually enhanced and reached a stable plateau within 24 min, implying that **PTMQ** took a relatively slow chemical reaction with N_2H_4. Therefore, it provides a temporal and spectral discriminative manner to determine N_2H_4 and ClO^-.

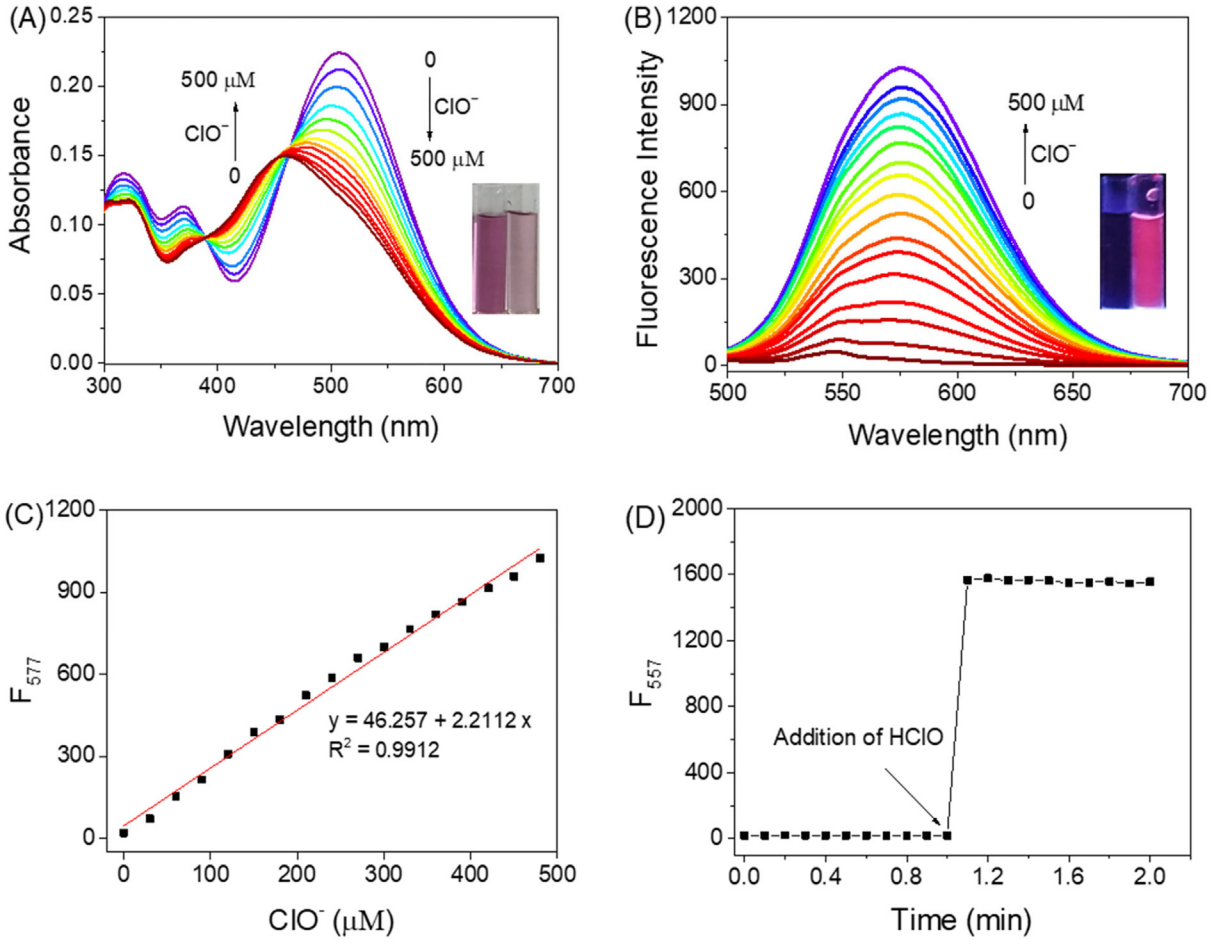

Fig. 1. (A) The UV–vis absorption spectra and (B) the fluorescence spectra of **PTMQ** (10 μM) upon addition of various concentrations of ClO^- (0–50 eq) in DMSO/PBS solution (v/v = 2:8, pH = 7.4). Inset: colorimetric or fluorescent responses of **PTMQ** towards ClO^- under daylight or 365 nm light. (C) The linear relationship between fluorescence intensity of **PTMQ** (10 μM) and concentrations of ClO^-. (D) Time-dependent fluorescence response of **PTMQ** (10 μM) to ClO^- (500 μM) in DMSO/PBS solution (v/v = 2/8, pH = 7.4). λ_{ex} = 460 nm, slits: 5 nm/5 nm.

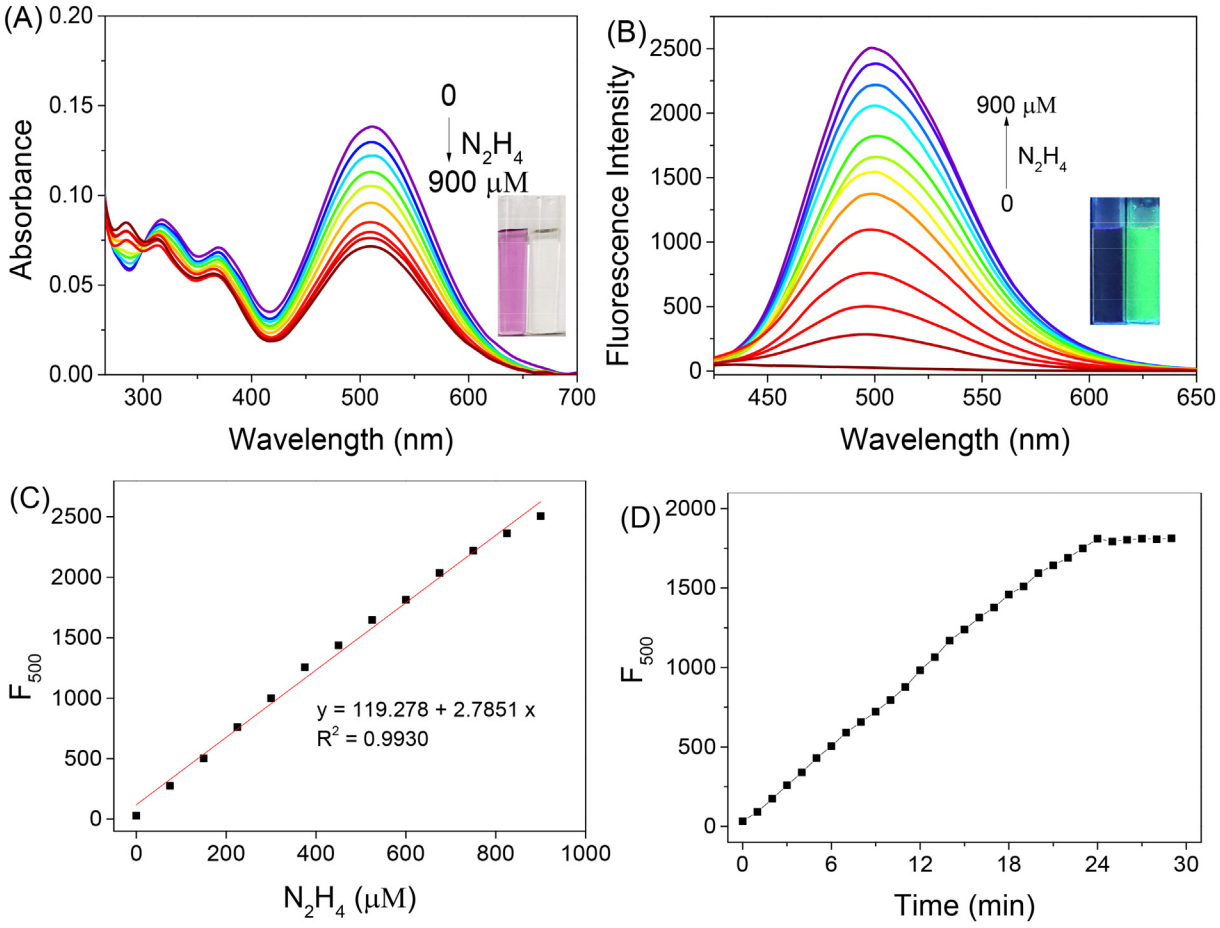

Fig. 2. (A) The UV–vis absorption spectra and (B) the fluorescence spectra of PTMQ (10 μM) upon addition of various concentrations of N_2H_4 (0–100 eq) in DMSO/PBS solution (v/v = 2:8, pH = 7.4). Inset: colorimetric or fluorescent responses of **PTMQ** towards N_2H_4 under daylight or 365 nm light. (C) The linear relationship between fluorescence intensity of **PTMQ** (10 μM) and concentrations of N_2H_4. (D) Time-dependent fluorescence response of **PTMQ** (10 μM) to N_2H_4 (900 μM) in DMSO/PBS solution (v/v = 2/8, pH = 7.4). λ_{ex} = 360 nm, slits: 2.5 nm/5 nm.

3.3. Effect of pH on the sensing performance

As an important environmental factor, pH value usually has a large impact on the chemical stability and sensing capability of fluorescence probes [31]. Herein, the pH-dependent fluorescence response of **PTMQ** (10 μM) to ClO^- (500 μM) and N_2H_4 (900 μM) were investigated, respectively. As depicted in Fig. 3A, the fluorescence intensity at 577 nm (F_{577}) of **PTMQ** almost maintained constant within the pH range of 3.0–9.5. Upon the addition of ClO^- (500 μM) to **PTMQ** solution, an obvious fluorescence enhancement was observed at pH 5.0–8.5. Whereas, the fluorescence intensity at 500 nm (F_{500}) of **PTMQ** also kept constant within the pH range of 3.0–10.0, as shown in Fig. 3B. The addition of N_2H_4 (900 μM) also led to a sharp fluorescence enhancement at pH 6.0–9.5. Therefore, **PTMQ** itself owns good pH stability and remarkable fluorescence response to ClO^- and N_2H_4 at pH 7.4, which is suitable for intracellular bioimaging applications.

3.4. The selectivity

For practical detection, a favorable fluorescent probe should have high selectivity to the analyte. Herein, we tested the selectivity of **PTMQ** (10 μM) to ClO^- (500 μM), N_2H_4 (900 μM) and various species

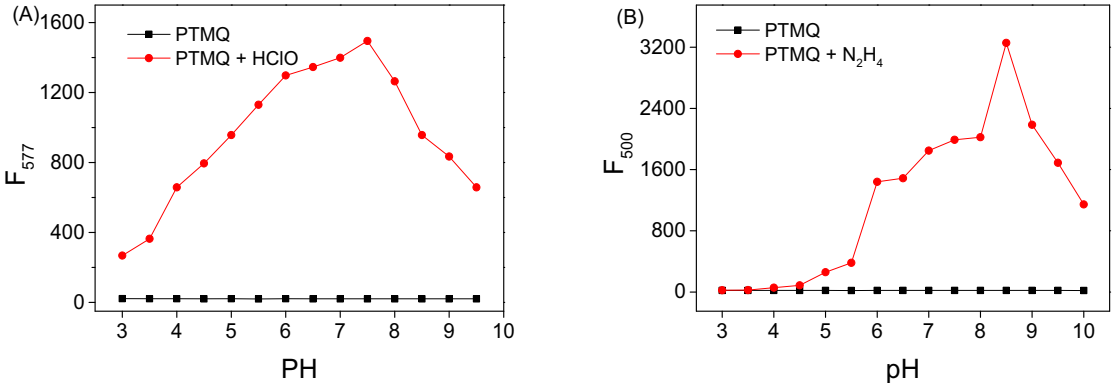

Fig. 3. Fluorescence intensity of **PTMQ** (10 μM) to (A) ClO^- (λ_{ex} = 460 nm, slits: 5 nm/5 nm) and (B) N_2H_4 (λ_{ex} = 360 nm, slits: 2.5 nm/5 nm) in DMSO/PBS solution (v/v = 2/8) at various pH values.

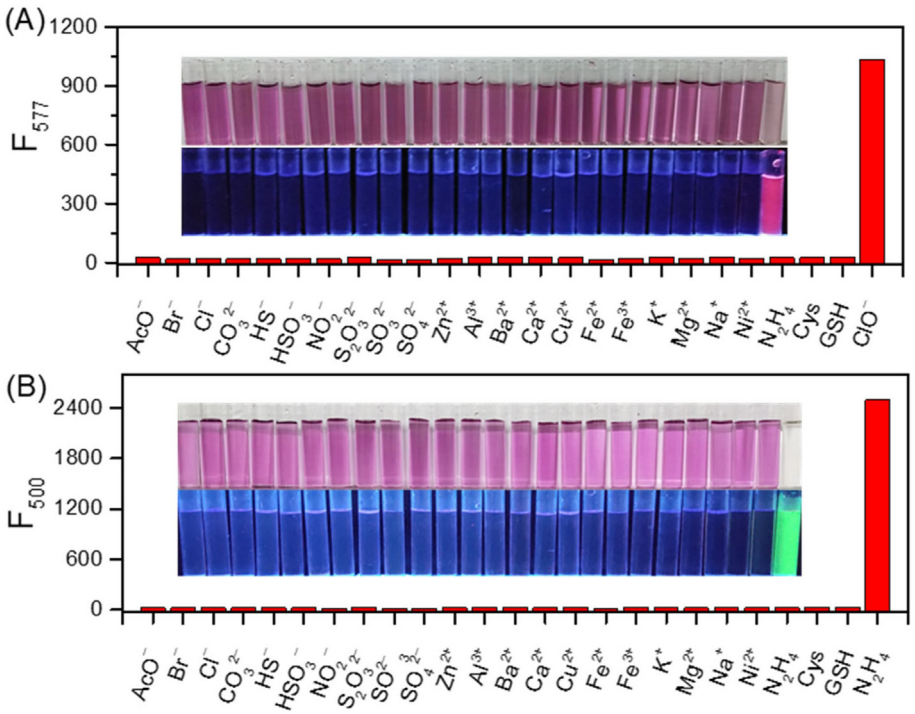

Fig. 4. (A) The fluorescent responses of **PTMQ** (10 μM) to ClO^- (500 μM) and other analytes (500 μM). λ_{ex} = 460 nm, slits: 5 nm/5 nm; (B) The fluorescent responses of **PTMQ** (10 μM) to N_2H_4 (900 μM) and other biological molecular species (900 μM). λ_{ex} = 360 nm, slits: 2.5 nm/5 nm. Inset: Color and fluorescence photograms of **PTMQ** (10 μM) in the presence of various analytes.

including anions (AcO^-, Br^-, Cl^-, CO_3^{2-}, HS^-, HSO_3^-, NO_2^-, $S_2O_3^{2-}$, SO_3^{2-} and SO_4^{2-}), metal cations (Zn^{2+}, Al^{3+}, Ba^{2+}, Ca^{2+}, Cu^{2+}, Fe^{2+}, Fe^{3+}, K^+, Mg^{2+}, Na^+, Ni^{2+}) as well as biothiols (Cys and GSH). As shown in Fig. 4A, negligible fluorescence and color changes of **PTMQ** were observed in the presence of various species except ClO^-. In contrast, the addition of ClO^- brought an evident bathochromic shift from purple to light pink with an obvious fluorescence enhancement at 577 nm. Likewise, **PTMQ** (10 μM) also demonstrated remarkable green fluorescence "turn-on" response to N_2H_4 (100 μM) along with color change from purple to colorless (Fig. 3B). The results indicated that probe **PTMQ** possesses excellent selectivity to ClO^- and N_2H_4, which might be employed as a potential tool for real sample detection.

3.5. Working mechanism

To further understand the working mechanism, we made great efforts to isolate the major products generated from the reactions of **PTMQ** with ClO^- and N_2H_4, respectively. Unfortunately, we could not obtain the pure products for NMR analysis due to their strong polarity and some complex fragments. So, we can only measure the HRMS spectra of main products. After **PTMQ** was treated with ClO^-, the HRMS spectra of **PTMQ** (Fig. S8) showed a dominant peak located at *m/z* value of 465.1649 (calcd: 465.1612), which was corresponding to [**PTMQ**-O^+]. It was proposed that the electron-donating sulfur atom (—S—) in phenothiazine was converted into electron-withdrawing sulfoxide (-S=O) group after reaction with ClO^- [30], which blocked the intramolecular charge transfer effect (ICT), and thus leading to a significant red fluorescence enhancement. For the sensing mechanism of N_2H_4, the HRMS spectra (Figs. S9 and S10) showed two main peaks at m/z values of 310.1026 and 172.1146 after reaction with N_2H_4, which were identified as **PT-NHNH$_2$** (calcd: 310.1051) and **MQ** (calcd: 172.1027), respectively. These observations indicated that the polarized C=C bridge of **PTMQ** could be disrupted by nucleophilic N_2H_4 to form **PT-NHNH$_2$** [17], which gave rise to green fluorescence emission. Based on these observations, the proposed working mechanisms of **PTMQ** for HClO/ClO^- and N_2H_4 were depicted in Scheme 2.

3.6. Cell imaging

In view of the aforementioned excellent sensing properties, **PTMQ** was utilized to separately image HClO and N_2H_4 in human cervical cancer (HeLa) cells [32,33]. Firstly, the HeLa cells were pre-incubated with **PTMQ** (10 μM) at 37 °C for 30 min, and the fluorescence images were recorded by laser confocal scanning microscopy. As illustrated in Fig. 5A and B, for the blank cells, non-fluorescence could be observed in red and green channels. Then, these HeLa cells were co-incubated with different amounts of ClO^- (0, 80 and 200 μM) and N_2H_4 (0, 300, and 900 μM) for 30 min, and their fluorescence images were recorded.

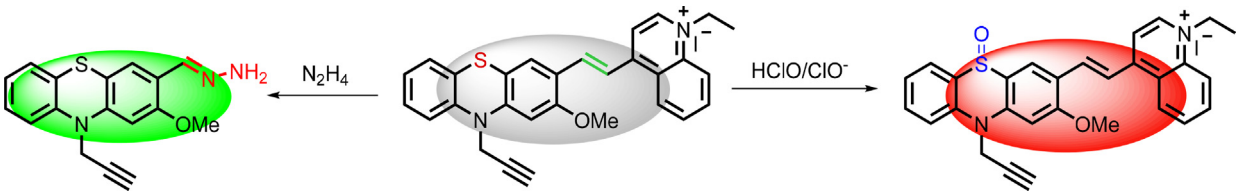

Scheme 2. The proposed mechanism of **PTMQ** for ClO^- and N_2H_4

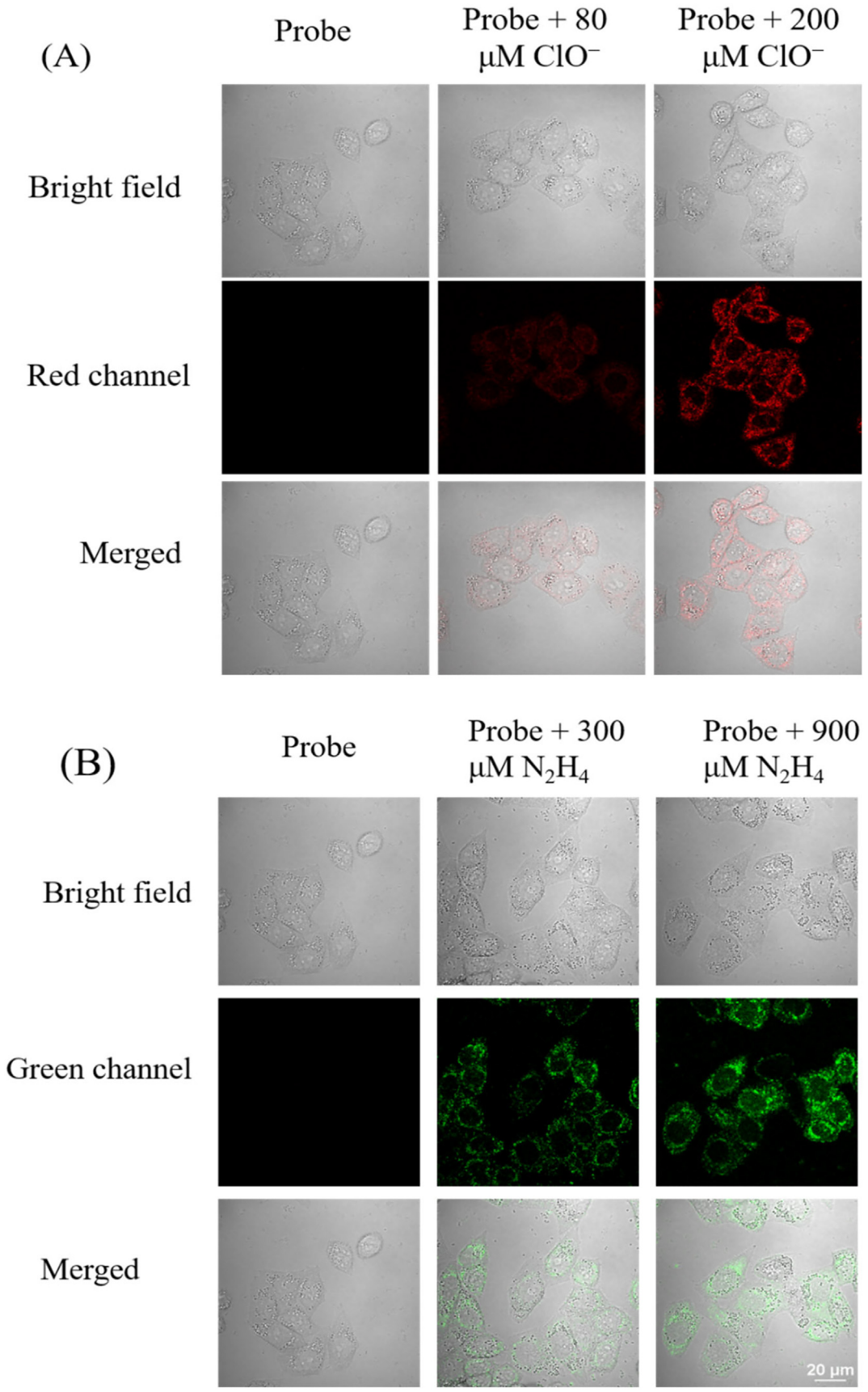

Fig. 5. Fluorescence images of living HeLa cells treated with ClO^- or N_2H_4. HeLa cells were pre- treated with **PTMQ** (10 μM) at 37 °C for 30 min, then washed with PBS and further co-incubated with different concentrations of (A) ClO^- (0, 80 and 200 μM), fluorescence images from the red channel (λ_{ex} = 543 nm, λ_{em} = 552–617 nm), and (B) N_2H_4 (0, 300 and 900 μM) for another 30 min, fluorescence images from the green channel (λ_{ex} = 488 nm, λ_{em} = 500–530 nm). Scale bar: 20 μm.

The cells after incubation with 80 μM of ClO^- displayed weak red fluorescence emission, which became much brighter with the increase of ClO^- concentration from 80 μM to 200 μM. By contrast, the cells showed clear green fluorescence at N_2H_4 concentration of 300 μM and remarkable green fluorescence emission when the concentration rose up to 900 μM. These observations demonstrated that **PTMQ** could serve as an efficient fluorescent probe for separately imaging of exogenous ClO^- and N_2H_4 in living cells. Moreover, it can be observed that the intracellular green/red fluorescence of **PTMQ** induced by ClO^- and N_2H_4 mainly localized in the cytoplasm within 30 min, suggesting that ClO^- and N_2H_4 can quickly penetrate and diffuse inside the HeLa cell, which may eventually cause oxidative-injury and/or hepatic steatosis [34]. The dual-analytes responsive properties, high contrast ratio, and low background interference, enable **PTMQ** to serve as a promising tool for discriminatively bioimaging and monitoring ClO^- and N_2H_4.

4. Conclusion

In conclusion, we have designed and synthesized a dual-analytes responsive fluorescent probe **PTMQ** for distinguishing detection of ClO^- and N_2H_4 in aqueous solution. **PTMQ** exhibited a colorimetric and ratiometric fluorescence response to N_2H_4 with good selectivity and a low detection limit (89 nM). Meanwhile, **PTMQ** displayed red fluorescence lighting-up response to ClO^- with good selectivity, rapid response (<0.2 min) and a low detection limit (58 nM). Moreover, **PTMQ** showed good biocompatibility and could be applied for in-situ imaging of ClO^- and N_2H_4 in living HeLa cells. This work provides an efficient way to create dual-analytes responsive fluorescent probe with the advantages of visual detection, good selectivity, as well as in situ discriminative bioimaging of two analytes in cancer cells.

CRediT authorship contribution statement

Beitong Zhu: Investigation, Writing - original draft. **Xiaoli Wu:** Methodology, Investigation, Data curation. **João Rodrigues:** Writing - review & editing. **Xichao Hu:** Methodology, Writing - original draft. **Ruilong Sheng:** Project administration, Writing - review & editing. **Guang-Ming Bao:** Conceptualization, Project administration, Supervision.

Declaration of competing interest

The authors declare that they have no known competing financial interests or personal relationships that could have appeared to influence the work reported in this paper.

Acknowledgements

This work was sponsored by the NSFC (no. 31960720), Fundação para a Ciência e a Tecnologia (FCT Base Fund - UIDB/00674/2020), ARDITI-Agência Regional para o Desenvolvimento da Investigação Tecnologia e Inovação through the project M1420-01-0145-FEDER-000005-Centro de Química da Madeira-CQM+ (Madeira 14-20 Program) and ARDITI-2017-ISG-003.

Appendix A. Supplementary data

Supplementary data to this article can be found online at https://doi.org/10.1016/j.saa.2020.118953.

References

[1] M. Annalakshmi, P. Balasubramanian, S.-M. Chen, T.-W. Chen, One pot synthesis of nanospheres-like trimetallic NiFeCo nanoalloy: a superior electrocatalyst for electrochemical sensing of hydrazine in water bodies, Sens. Actuators B Chem. 296 (2019) 126620.
[2] Z. Zhao, G. Zhang, Y. Gao, X. Yang, Y. Li, A novel detection technique of hydrazine hydrate: modality change of hydrogen bonding-induced rapid and ultrasensitive colorimetric assay, Chem. Commun. 47 (2011) 12816–12818.
[3] J. Mondal, A.K. Manna, K. Rout, S.K. Singh, J.P. Naskar, G.K. Patra, A simple Schiff base as selective and sensitive fluorescent-colorimetric hydrazine chemosensor, Int. J. Environ. Anal. Chem. 98 (2018) 1160–1174.
[4] J. Qian, C. Wen, J. Xia, Development of highly efficient chemosensors for Cu2+ and N2H4 detection based on 2D polyaniline derivatives by template-free chemical polymerization method, J. Hazard. Mater. 121902 (2019).
[5] N. Kwon, Y. Hu, J. Yoon, Fluorescent chemosensors for various analytes including reactive oxygen species, biothiol, metal ions, and toxic gases, ACS Omega 3 (2018) 13731–13751.
[6] J. Yan, S. Lee, A. Zhang, J. Yoon, Self-immolative colorimetric, fluorescent and chemiluminescent chemosensors, Chem. Soc. Rev. 47 (2018) 6900–6916.
[7] D. Wu, A.C. Sedgwick, T. Gunnlaugsson, E.U. Akkaya, J. Yoon, T.D. James, Fluorescent chemosensors: the past, present and future, Chem. Soc. Rev. 46 (2017) 7105–7123.
[8] M. Lan, S. Zhao, S. Wu, X. Wei, Y. Fu, J. Wu, P. Wang, W. Zhang, Optically tunable fluorescent carbon nanoparticles and their application in fluorometric sensing of copper ions, Nano Res. 12 (2019) 2576–2583.
[9] Y. Fu, S. Wu, H. Zhou, S. Zhao, M. Lan, J. Huang, X. Song, Carbon dots and a CdTe quantum dot hybrid-based fluorometric probe for spermine detection, Ind. Eng. Chem. Res. 59 (2020) 1723–1729.
[10] T. Xu, S. Zhao, X. Wu, L. Zeng, M. Lan, β-Cyclodextrin-promoted colorimetric and fluorescence turn-on probe for discriminating highly toxic thiophenol from biothiols, ACS Sustainable Chem. Eng. 8 (2020) 6413–6421.
[11] Y. Fu, S. Zhao, S. Wu, L. Huang, T. Xu, X. Xing, M. Lan, X. Song, A carbon dots-based fluorescent probe for turn-on sensing of ampicillin, Dyes Pigments 172 (2020) 107846.
[12] X.-X. Zheng, S.-Q. Wang, H.-Y. Wang, R.-R. Zhang, J.-T. Liu, B.-X. Zhao, Novel pyrazoline-based selective fluorescent probe for the detection of hydrazine, Spectrochim, Acta A 138 (2015) 247–251.
[13] L. Wang, F.-y. Liu, H.-y. Liu, Y.-s. Dong, T.-q. Liu, J.-f. Liu, Y.-w. Yao, X.-j. Wan, A novel pyrazoline-based fluorescent probe for detection of hydrazine in aqueous solution and gas state and its imaging in living cells, Sens. Actuators B Chem. 229 (2016) 441–452.
[14] R. Maji, A.K. Mahapatra, K. Maiti, S. Mondal, S.S. Ali, P. Sahoo, S. Mandal, M.R. Uddin, S. Goswami, C.K. Quah, H.-K. Fun, A highly sensitive fluorescent probe for detection of hydrazine in gas and solution phases based on the Gabriel mechanism and its bioimaging, RSC Adv. 6 (2016) 70855–70862.
[15] C. Hu, W. Sun, J. Cao, P. Gao, J. Wang, J. Fan, F. Song, S. Sun, X. Peng, A ratiometric near-infrared fluorescent probe for hydrazine and its in vivo applications, Org. Lett. 15 (2013) 4022–4025.
[16] G. Yu, Y. Cao, H. Liu, Q. Wu, Q. Hu, B. Jiang, Z. Yuan, A spirobenzopyran-based multifunctional chemosensor for the chromogenic sensing of Cu2+ and fluorescent sensing of hydrazine with practical applications, Sens. Actuators B Chem. 245 (2017) 803–814.
[17] J. Wu, J. Pan, Z. Ye, L. Zeng, D. Su, A smart fluorescent probe for discriminative detection of hydrazine and bisulfite from different emission channels, Sens. Actuators B Chem. 274 (2018) 274–284.
[18] J. Shepherd, S.A. Hilderbrand, P. Waterman, J.W. Heinecke, R. Weissleder, P. Libby, A fluorescent probe for the detection of myeloperoxidase activity in atherosclerosis-associated macrophages, Chem. Biol. 14 (2007) 1221–1231.
[19] Z.-N. Sun, F.-Q. Liu, Y. Chen, P.K.H. Tam, D. Yang, A highly specific BODIPY-based fluorescent probe for the detection of hypochlorous acid, Org. Lett. 10 (2008) 2171–2174.
[20] Y. Koide, Y. Urano, K. Hanaoka, T. Terai, T. Nagano, Development of an Si-rhodamine-based far-red to near-infrared fluorescence probe selective for hypochlorous acid and its applications for biological imaging, J. Am. Chem. Soc. 133 (2011) 5680–5682.
[21] S. Kenmoku, Y. Urano, H. Kojima, T. Nagano, Development of a highly specific rhodamine-based fluorescence probe for hypochlorous acid and its application to real-time imaging of phagocytosis, J. Am. Chem. Soc. 129 (2007) 7313–7318.
[22] W. Lin, L. Long, B. Chen, W. Tan, A ratiometric fluorescent probe for hypochlorite based on a deoximation reaction, Chem. Eur. J. 15 (2009) 2305–2309.
[23] X. Cheng, H. Jia, T. Long, J. Feng, J. Qin, Z. Li, A "turn-on" fluorescent probe for hypochlorous acid: convenient synthesis, good sensing performance, and a new design strategy by the removal of C═N isomerization, Chem. Commun. 47 (2011) 11978–11980.
[24] G. Cheng, J. Fan, W. Sun, K. Sui, X. Jin, J. Wang, X. Peng, A highly specific BODIPY-based probe localized in mitochondria for HClO imaging, Analyst 138 (2013) 6091–6096.
[25] Y.-K. Yang, H.J. Cho, J. Lee, I. Shin, J. Tae, A rhodamine–hydroxamic acid-based fluorescent probe for hypochlorous acid and its applications to biological imagings, Org. Lett. 11 (2009) 859–861.
[26] Q. Hu, C. Qin, L. Huang, H. Wang, Q. Liu, L. Zeng, Selective visualization of hypochlorite and its fluctuation in cancer cells by a mitochondria-targeting ratiometric fluorescent probe, Dyes Pigments 149 (2018) 253–260.
[27] J. Zha, B. Fu, C. Qin, L. Zeng, X. Hu, A ratiometric fluorescent probe for rapid and sensitive visualization of hypochlorite in living cells, RSC Adv. 4 (2014) 43110–43113.
[28] J.-T. Hou, H.S. Kim, C. Duan, M.S. Ji, S. Wang, L. Zeng, W.X. Ren, J.S. Kim, A ratiometric fluorescent probe for detecting hypochlorite in the endoplasmic reticulum, Chem. Commun. 55 (2019) 2533–2536.
[29] A.J. Winstead, G. Nyambura, R. Matthews, D. Toney, S. Oyaghire, Synthesis of quaternary heterocyclic salts, Molecules 18 (2013) 14306–14319.
[30] H. Song, Y. Zhou, C. Xu, X. Wang, J. Zhang, Y. Wang, X. Liu, M. Guo, X. Peng, A dual-function fluorescent probe: sensitive detection of water content in commercial

products and rapid detection of hypochlorite with a large Stokes shift, Dyes Pigments 162 (2019) 160–167.
[31] X. Wu, L. Zeng, B.-Q. Chen, M. Zhang, J. Rodrigues, R. Sheng, G.-M. Bao, A selective cascade reaction-based probe for colorimetric and ratiometric fluorescence detection of benzoyl peroxide in food and living cells, J. Mater. Chem. B 7 (2019) 5775–5781.
[32] Z. Ye, C. Duan, R. Sheng, J. Xu, H. Wang, L. Zeng, A novel colorimetric and ratiometric fluorescent probe for visualizing SO2 derivatives in environment and living cells, Talanta 176 (2018) 389–396.
[33] J. Xu, Y. Zhang, L. Zeng, J. Liu, J.M. Kinsella, R. Sheng, A simple naphthalene-based fluorescent probe for high selective detection of formaldehyde in toffees and HeLa cells via aza-cope reaction, Talanta 160 (2016) 645–652.
[34] S. Garrod, M.E. Bollard, A.W. Nicholls, S.C. Connor, J. Connelly, J.K. Nicholson, E. Holmes, Integrated metabonomic analysis of the multiorgan effects of hydrazine toxicity in the rat, Chem. Res. Toxicol. 18 (2005) 115–122.